Cluster-Based Multi-Objective Optimization of Surface Roughness in Dry Machining of Ti6Al4V: A Data-Driven Approach for Industrial Parameter Selection

Alex Fernandes de Souza (Universidade Federal de Itajubá) *alex_fernandes1989@live.com*
Pedro Paulo Balestrassi (Universidade Federal de Itajubá) *pedro@unifei.edu.br*

Abstract

Machining Ti-6Al-4V under dry conditions poses major challenges due to its low thermal conductivity, high chemical reactivity, and strong sensitivity of surface roughness to cutting parameters. Conventional optimization approaches often fail to capture the nonlinear and heterogeneous nature of this process, leading to suboptimal industrial recommendations. This study proposes a cluster-based multi-objective optimization framework for selecting cutting parameters in dry machining of Ti-6Al-4V, aiming to minimize surface roughness while accounting for cutting forces and process reliability. A dataset comprising 287 dry orthogonal cutting experiments was analyzed, covering a wide range of cutting speeds and feed rates. K-means clustering was applied to identify distinct operational regimes, revealing three machining clusters: Conventional, High-Feed, and High-Speed. Within each cluster, second-order response surface models were fitted for surface roughness and cutting force, and a weighted multi-objective function was optimized to determine regime-specific parameter recommendations. A data-driven success criterion, based on surface roughness and tool-wear state, was used to evaluate process reliability. The results show that the Conventional cluster provides the highest reliability (92.2% success rate) with stable surface quality, while the High-Feed cluster achieves higher productivity and slightly lower roughness at the expense of increased cutting forces and reduced reliability. The High-Speed cluster exhibited limited robustness and did not support stable optimization due to data sparsity and strong nonlinearities. Overall, the cluster-based approach outperformed global optimization by capturing distinct machining regimes and enabling tailored industrial parameter selection.

Keywords: *Ti-6Al-4V, Dry machining, Surface roughness, Clustering, Multi-objective optimization.*

1. Introduction

Machining Ti6Al4V poses significant challenges in aerospace and biomedical industries due to its low thermal conductivity and high strength at elevated temperatures. Dry machining exacerbates difficulties in controlling surface finish and tool wear. Surface roughness, critical for high-precision parts, is influenced by cutting parameters through complex, non-linear relationships that are often oversimplified in traditional empirical or analytical models.

Data-driven methods in smart manufacturing offer potential solutions, but high experimental variability and non-linear parameter-response relationships hinder standard optimization. Ti6Al4V machining involves multiple interacting surface-formation mechanisms, and the lack of reliable predictive models limits the implementation of strategies that balance productivity, surface quality, and process reliability.

Existing studies on cutting parameters and surface roughness often assume monotonic or linear trends, leading to suboptimal recommendations that ignore distinct machining regimes. Furthermore, most approaches focus on single-objective optimization without properly addressing the trade-offs among surface quality, cutting forces, and process stability.

Cluster analysis provides a robust framework to uncover inherent patterns in machining data, identifying natural groupings that represent different operational regimes. This approach reveals relationships not captured by conventional statistics and enables tailored optimization strategies for each regime, moving beyond generic "one-size-fits-all" solutions.

Given this context, this study aims to develop and validate a cluster-based multi-objective optimization methodology for dry machining of Ti6Al4V, focusing on minimizing surface roughness while accounting for cutting forces and process stability. Specifically, it seeks to identify distinct operational regimes through cluster analysis, determine optimal parameters for each regime, and provide practical, evidence-based recommendations for industrial parameter selection.

2. Theoretical Background

The formation of surface roughness during dry machining of Ti-6Al-4V arises from the coupled effects of tool geometry, cutting kinematics, material behavior, and thermo-mechanical interactions at the tool–chip interface. In a data-driven modeling context, this relationship is commonly represented by a nonlinear response surface linking the cutting parameters to the surface roughness (Souza et al., 2026). As expressed in Equation (1), the average roughness is modeled as a second-order polynomial of the cutting parameters.

$$\mathrm{R_a(x)} = \beta_0 + \boldsymbol{\beta}^{\mathrm{T}}\mathrm{x} + \mathrm{x}^{\mathrm{T}}\mathbf{B}\mathrm{x} + \varepsilon \quad (1)$$

Where $x = [v_c, f, a_p]^T$ is the vector of cutting parameters, $\boldsymbol{\beta}$ is the vector of linear coefficients, $\mathbf{B}$ is the symmetric matrix containing quadratic and interaction terms, and ε represents experimental noise (Amaral et al., 2023). This formulation allows the model to capture both curvature and parameter interactions, which are critical for representing the highly nonlinear surface formation mechanisms in Ti-6Al-4V machining.

From a purely kinematic standpoint, surface roughness is primarily governed by feed rate and tool geometry. Under ideal conditions, the theoretical roughness can be approximated by Equation (2) (Liu et al., 2024).

$$R_{a,geo} \approx f^2 / (32\, r_\varepsilon) \quad (2)$$

Where f is the feed rate and r_ε is the tool nose radius. However, during dry machining of Ti-6Al-4V, this geometric baseline is significantly modified by thermal softening, adhesion, tool wear, and dynamic instabilities. Consequently, the effective surface roughness deviates from Equation (2), and these deviations are implicitly captured by the regression-based formulation in Equation (1).

Cutting force plays a central role in process stability, tool loading, and surface integrity. In machining science, it is commonly described using a multiplicative power-law model, as given by Equation (3) (Chen et al., 2022).

$$Fc = K \cdot a_p{}^{\alpha} \cdot f^m \cdot v_c{}^n \quad (3)$$

Where K, α, m, and n are material- and process-dependent constants. This formulation reflects the physical fact that chip load increases primarily with feed rate and depth of cut, while cutting speed modulates strain-rate sensitivity and thermal effects. Equation (3) therefore provides a physically meaningful link between cutting parameters and mechanical loading.

Although global regression models can represent average trends, Ti-6Al-4V machining is characterized by the existence of multiple operational regimes, each associated with different chip-formation modes, thermal states, and stability conditions (Sharma et al., 2022). To identify such regimes, unsupervised learning is employed through K-means clustering, which minimizes the within-cluster variance as expressed in Equation (4).

$$J = \sum_{i=1}^{k} \sum_{z \in C_i} || z - \mu_i ||^2 \tag{4}$$

Where C_i denotes the i-th cluster and μ_i is its centroid. This formulation groups machining conditions that exhibit similar combinations of roughness, force, and stability, thereby defining distinct cutting regimes within the experimental domain.

Once the clusters are identified, regime-dependent models can be constructed, yielding response functions $R_a(x \mid c)$ and $F_c(x|c)$. This approach allows the optimization process to be performed locally within each cluster, ensuring that parameter recommendations are consistent with the underlying physical and statistical behavior of that regime.

The industrial selection of cutting parameters is inherently multi-objective, since reductions in surface roughness often conflict with increases in cutting force (Nguyen et al., 2023). This trade-off is expressed by the vector objective function given in Equation (5).

$$f(x) = [\, R_a(x),\, F_c(x)\,]^T \tag{5}$$

For practical implementation, the multi-objective problem can be reduced to a scalar cost function through weighted aggregation, as shown in Equation (6).

$$\Phi(x) = w_1 \tilde{}R_a(x) + w_2 \tilde{}F_c(x), \; w_1 + w_2 = 1 \tag{6}$$

Where $\tilde{}R_a$ and $\tilde{}F_c$ denote normalized responses. Equation (6) formalizes the compromise between surface quality and mechanical load, enabling objective and reproducible selection of cutting parameters within each cluster-defined machining regime.

3. Methodology

3.1 Experimental Data Source

The dataset used in this study was obtained from the large-scale dry orthogonal cutting experiments conducted by Klippel et al. (2024) on Ti-6Al-4V alloy. The material consisted of 6 wt.% aluminum and 4 wt.% vanadium, with α (hcp) and β (bcc) phases. Thin-walled cylindrical specimens (72 mm diameter and 2 mm wall thickness) were machined on a Schaublin 42 L CNC lathe.

A fractional factorial design was adopted, comprising 26 cutting speed levels (10–500 m/min) and 11 feed levels (0.01–0.40 mm/rev), resulting in 109 parameter combinations and 287 experiments with 2–3 replications. The depth of cut was kept constant under quasi-orthogonal cutting conditions. Cutting forces were measured using a Kistler 9121A5 dynamometer, filtered at 30 Hz and sampled at 1.1 kHz, with analysis focused on the main cutting force component F_c. Tool wear of Sandvik Coromant CCMW 09T304 H13A inserts was classified as Low (L), Medium (M), or High (H). Table 1 summarizes the cutting parameters, their levels, and the experimental scope of the dataset.

Table 1 – Experimental design and cutting parameter ranges used in the Ti-6Al-4V machining tests.

Parameter	Levels	Range
Cutting speed (vc, m/min)	26	10–500
Feed (f, mm/rev)	11	0.01–0.40
Tested combinations	109	–
Replications	2–3	–
Total experiments	287	–

Source: Adapted from Klippel et al. (2024).

A trial success indicator was defined to quantify the feasibility and reliability of each machining condition. A trial i was classified as successful when it met an acceptable surface-quality requirement and did not present severe tool degradation, as defined in Equation (11).

$$S_i = \begin{cases} 1, & if\ R_{a,i} \leq R_a^{thr}\ and\ W_i \neq High, \\ 0, & otherwise, \end{cases} \tag{11}$$

Where Si is the binary success indicator for trial i, Ra,i is the measured surface roughness, Wi is the qualitative tool-wear label (Low, Medium, High), and Ra^thr is the roughness threshold. In this study, Ra^thr was set to the dataset median roughness (36.7 µm) to ensure a data-driven and non-arbitrary criterion. The success rate for each cluster was then computed as the percentage of trials with Si = 1.

3.2 Cluster Identification

Operational machining regimes were identified using K-means clustering applied to the normalized dataset. The clustering process minimizes the within-cluster variance, as defined in Equation (7).

$$J = \Sigma_{i=1}{}^{k} \Sigma_{x \in C_i} \parallel x - \mu_i \parallel^2 \tag{7}$$

Where x denotes the normalized feature vector, C_i is the i-th cluster, and μ_i is its centroid. Based on this formulation, experiments with similar thermo-mechanical behavior are grouped into distinct operational regimes. In this study, clusters were defined as high-speed ($v_c > 250$ m/min), high-feed ($f > 0.15$ mm/rev), and conventional cutting.

3.3 Cluster-Based Modeling

Within each cluster, surface roughness was modeled by a second-order response surface, as given in Equation (8), following standard response surface modeling approaches for Ti6Al4V machining (Gutema; Gopal; Lemu, 2026).

$$R_a = \beta_0 + \beta_1 v_c + \beta_2 f + \beta_{11} v_c^2 + \beta_{22} f^2 + \beta_{12} v_c f + \varepsilon \tag{8}$$

Where R_a denotes the arithmetic mean surface roughness, v_c is the cutting speed, f is the feed rate, β_i are regression coefficients, and ε represents experimental error.

Similarly, the cutting force was modeled by a quadratic polynomial, as shown in Equation (9).

$$F_c = \gamma_0 + \gamma_1 v_c + \gamma_2 f + \gamma_{11} v_c^2 + \gamma_{22} f^2 + \gamma_{12} v_c f + \varepsilon \tag{9}$$

Where F_c is the main cutting force and γ_i are regression coefficients.

3.4 Multi-Objective Optimization

The optimal cutting parameters for each cluster were obtained by minimizing the aggregated objective function given in Equation (10), following standard weighted-sum multi-objective optimization approaches widely adopted in machining and manufacturing optimization (Nguyen et al., 2023; Sharma et al., 2022). This formulation enables the simultaneous consideration of surface quality and mechanical loading, two competing objectives that strongly influence process performance and tool life in Ti-6Al-4V dry turning.

$$\Phi(\mathrm{x}) = w_1 \frac{R_a(x) - R_a^{min}}{R_a^{max} - R_a^{min}} + w_2 \frac{F_c(x) - F_c^{min}}{F_c^{max} - F_c^{min}} \tag{10}$$

Where w_1 and w_2 are weighting coefficients satisfying $w_1 + w_2 = 1$, and R_a^{min}, R_a^{max}, F_c^{min}, F_c^{max} denote the minimum and maximum values observed within each cluster. The normalization ensures that both objectives contribute comparably to the aggregated cost function, preventing dominance of either roughness or cutting force due to scale differences.

In this study, the weights were set to $w_1 = 0.7$ and $w_2 = 0.3$, reflecting the industrial priority given to surface finish in applications such as aerospace and biomedical components, while still accounting for tool loading and process stability. The optimization was performed independently within the parameter bounds of each cluster using the L-BFGS-B algorithm, which efficiently handles nonlinear objective functions with bounded constraints. This cluster-wise optimization strategy ensures that the resulting parameter recommendations remain physically meaningful and consistent with the local machining regime, avoiding unrealistic extrapolations that often arise from global optimization approaches.

4. Results and Discussion

The 287 experiments covered a wide range of cutting conditions, as summarized in Table 1. Cutting speed varied from 10 to 500 m/min (mean 118.4 m/min, CV = 98.8%), intentionally ensuring high variability to capture different machining regimes. Feed ranged from 0.01 to 0.40 mm/rev (mean 0.098 mm/rev, CV = 85.1%). Surface roughness (r_n) ranged from 23.8 to 46.8 µm (mean 36.7 µm, CV = 11.0%), showing relatively low dispersion despite the large variation in input parameters.

Table 2 - Descriptive statistics of the main study variables**.**

Variable	Mean	Std. Dev.	Min	Max	CV (%)	n
vc (m/min)	118.40	116.94	10.00	500.00	98.8	287
f (mm/rev)	0.098	0.083	0.01	0.40	85.1	287
rn (µm)	36.74	4.06	23.80	46.80	11.0	287
Fc (N)	180.18	112.04	−7.80	491.30	62.2	287
Ff (N)	129.45	54.93	−11.70	603.50	42.4	287
lcut (mm)	2903.08	1116.89	607.00	11136.00	38.5	287

Note: CV = coefficient of variation; negative force values result from measurement noise.
Source: Adapted from Klippel et al. (2024).

The accumulated cutting length (Icut) varied widely, reflecting different test durations and tool wear states. Some negative values of cutting and feed forces were observed due to sensor noise or calibration drift and were treated using absolute values for visualization. The intentionally high variability of cutting speed and feed (CV > 85%) supports the use of robust analytical methods capable of handling heterogeneous machining data.

As summarized in Table 2, the dataset exhibits high variability in both cutting speed and feed rate, which is visually confirmed by the distributions shown in Figure 1, highlighting the heterogeneous nature of the experimental space.

Figure 1 - Distributions of cutting speed, feed rate, surface roughness, and cutting force for the 287 experiments.

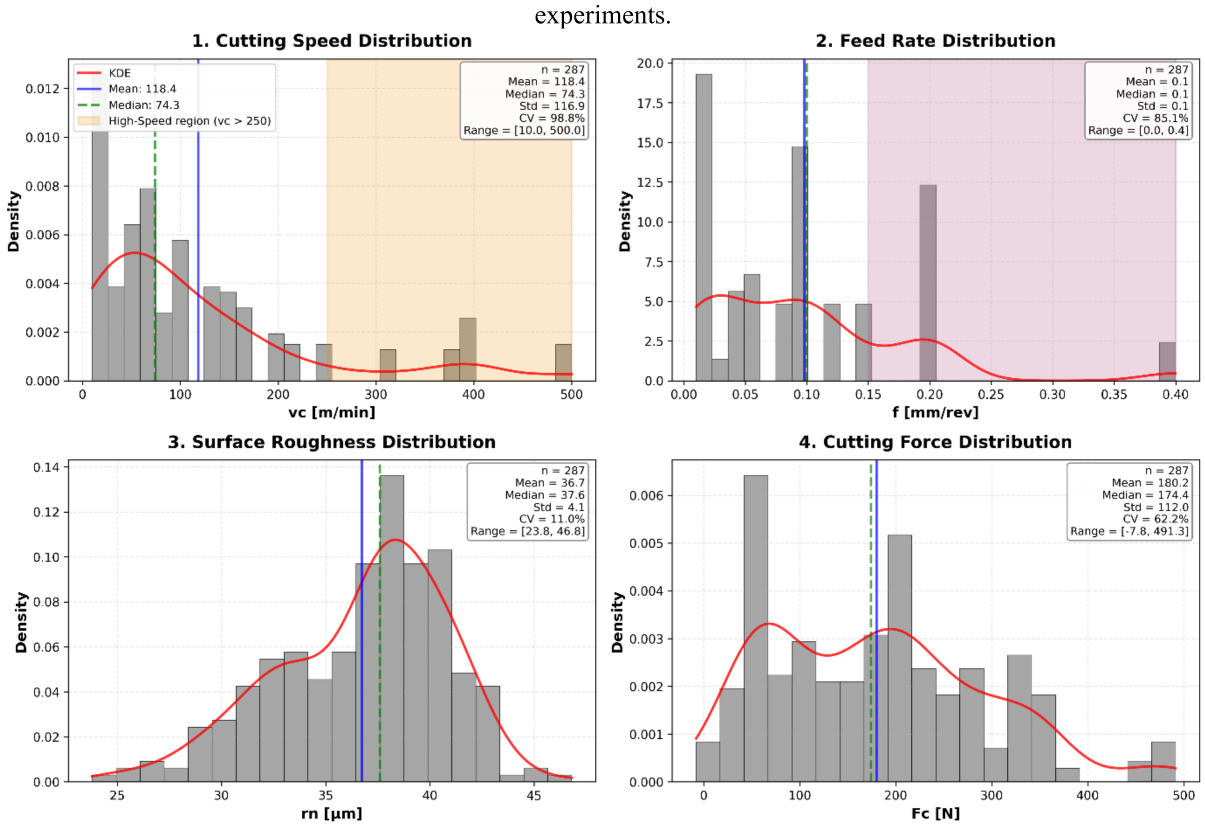

Source: Authors (2026).

Pearson correlation analysis revealed complex and often non-intuitive relationships among variables. As shown in Figure 2, surface roughness (rn) exhibited a moderate positive correlation with cutting length (r = 0.492), indicating the influence of progressive tool wear on surface quality. In contrast, both cutting speed (r = −0.034) and feed (r = −0.127) showed weak negative correlations with roughness, suggesting that higher values of these parameters do not necessarily degrade surface finish in dry machining of Ti-6Al-4V.

Figure 1 shows the distributions of cutting speed, feed rate, surface roughness, and cutting force for the 287 experimental trials. The cutting speed and feed rate histograms exhibit broad and asymmetric distributions, confirming that the experimental design intentionally covered a wide operational domain rather than concentrating around a narrow nominal setting. In contrast, surface roughness presents a more compact distribution, indicating that large variations in input parameters do not translate linearly into proportional changes in surface quality. The cutting force distribution is notably skewed, with long tails toward high values, reflecting the presence of localized high-load regimes. Together, these distributions provide strong evidence of data heterogeneity and motivate the need for cluster-based and nonlinear modeling approaches.

Figure 2 - Pearson correlation matrix of the main study variables. Color intensity indicates correlation magnitude, with positive values in blue and negative values in red.

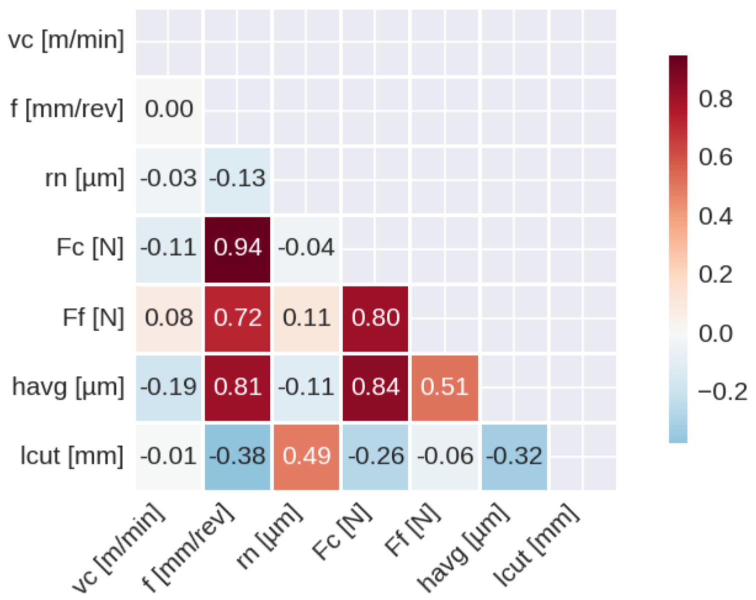

Source: Authors (2026).

Cutting force (Fc) showed a strong positive correlation with feed ($r = 0.746$), consistent with the increase in chip load. However, the correlation between force and roughness was weak and negative ($r = -0.039$), contradicting the assumption that higher forces necessarily worsen surface finish. This behavior indicates the coexistence of competing mechanisms, such as adhesion, built-up edge, and thermal effects, in surface formation.

The low magnitude of most correlations ($|r| < 0.5$, except for lcut) highlights the limitations of global linear models for this system. This finding supports the adoption of cluster-based and nonlinear approaches capable of capturing distinct machining regimes that are not visible in global correlation analysis.

Cluster analysis revealed three distinct operational regimes in the parameter space, as summarized in Table 3. The Conventional cluster (n = 204) exhibited a mean cutting speed of 76.6 m/min and a feed of 0.071 mm/rev, representing typical Ti-6Al-4V machining conditions. The High-Feed cluster (n = 45) was characterized by a significantly higher feed (0.222 mm/rev) with moderate cutting speed (90.6 m/min), corresponding to high-productivity strategies. The High-Speed cluster (n = 38) was dominated by extreme cutting speeds (mean 375.8 m/min) with variable feed, representing high-speed machining conditions.

Table 3 - Statistical characteristics of the three identified operational clusters.

Cluster	n	vc (m/min)	f (mm/rev)	Rn (µm)	Fc (N)	Success rate (%)
Conventional	204	76.6 ± 54.0	0.071 ± 0.044	37.25 ± 3.88	147.8 ± 77.5	92.2
High Feed	45	90.6 ± 62.7	0.222 ± 0.064	35.21 ± 4.64	352.2 ± 51.7	62.2
High Speed	38	375.8 ± 80.3	0.098 ± 0.124	35.78 ± 3.70	150.2 ± 135.0	55.3

Figure 3 illustrates the spatial distribution of the clusters in the speed–feed plane, revealing natural groupings that correspond to different operational philosophies. Notably, the High-Feed cluster exhibited the lowest mean surface roughness (35.21 µm), challenging the conventional assumption that higher feed rates necessarily degrade surface finish. However, this improvement in surface quality is achieved at the expense of substantially higher cutting forces (352.2 N versus 147.8 N in the Conventional cluster) and a significantly lower success rate (62.2% versus 92.2%).

Figure 3 - Distribution of surface roughness (Ra) across the three operational clusters (Conventional, High-Feed, and High-Speed), showing median, interquartile range, and dispersion of measurements.

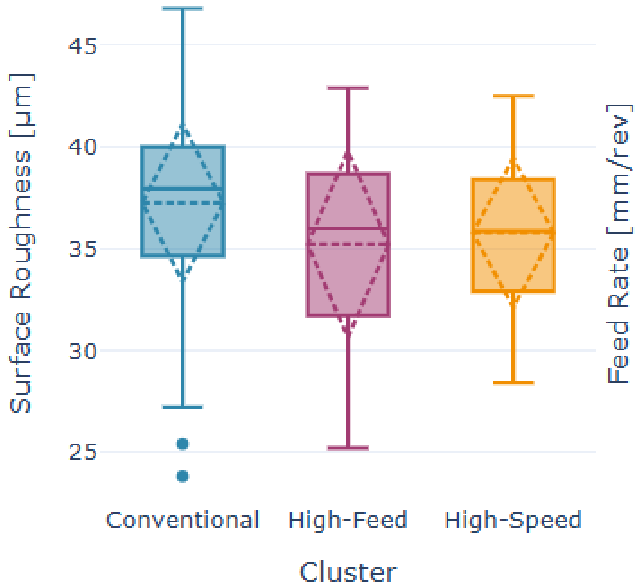

Source: Authors (2026).

The High-Speed cluster, although showing roughness comparable to the High-Feed cluster (35.78 µm), presented the lowest success rate (55.3%), indicating that extreme cutting speeds introduce additional process instabilities. The high variability in cutting force within this cluster (standard deviation 135.0 N) supports this interpretation, suggesting less predictable behavior under high-speed conditions.

Independent optimization for each cluster produced regime-specific parameter recommendations. For the Conventional cluster, the optimal parameters were vc = 70.0 m/min and f = 0.080 mm/rev, yielding predicted roughness between 34.8 and 37.6 µm. These values were validated by the nearest experimental trials (V0405–V0407), which showed roughness between 33.9 and 36.6 µm with "ok" status.

Independent optimization for each cluster produced regime-specific parameter recommendations. For the Conventional cluster, the optimal parameters were vc = 70.0 m/min and f = 0.080 mm/rev, yielding predicted roughness between 34.8 and 37.6 µm. These values were validated by the nearest experimental trials (V0405–V0407), which showed roughness between 33.9 and 36.6 µm with "ok" status.

As illustrated in Figure 4, the three-dimensional distribution of cutting speed, feed rate, and surface roughness reveals a highly structured experimental space, with clusters and gradients that reflect distinct machining regimes.

Figure 4 - Three-dimensional distribution of cutting speed, feed rate, and surface roughness for all experimental trials, showing the spatial structure of the dataset

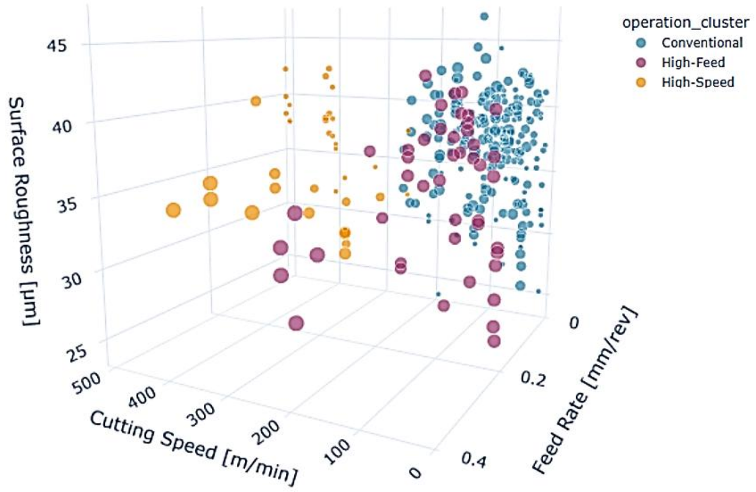

Source: Authors (2026).

For the High-Feed cluster, optimization converged to vc = 80.0 m/min and f = 0.200 mm/rev. The predicted roughness range (35.2–39.8 µm) was consistent with nearby experiments, although with greater dispersion (37.7–41.8 µm). Figure 5 presents the response surface for this cluster, highlighting the identified optimal region.

Figure 5 - Response surface of the objective function for the High-Feed cluster, with the optimal point indicated.

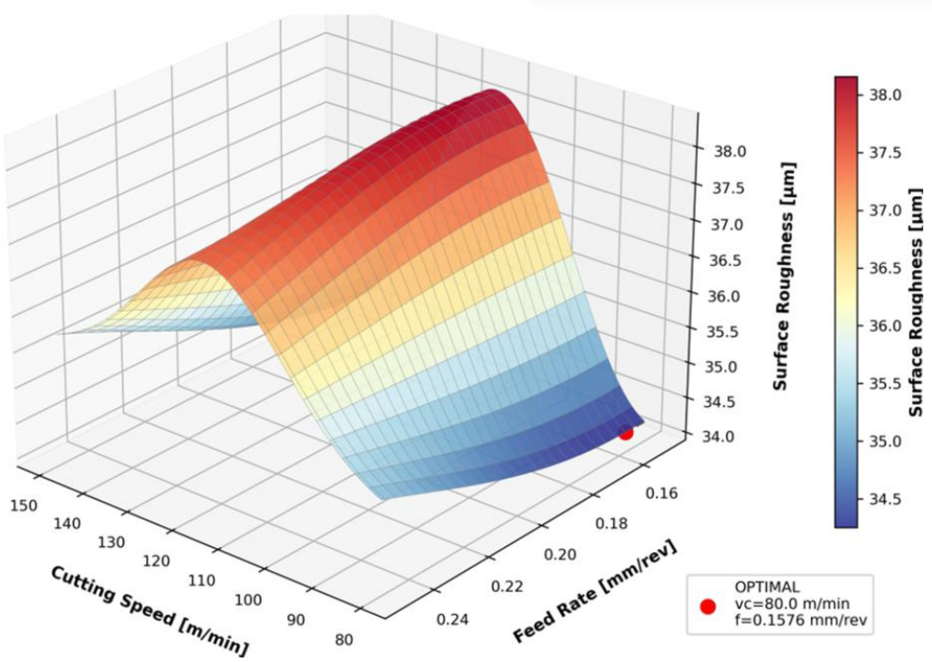

Source: Authors (2026).

As shown in Figure 5, the High-Feed cluster exhibits a smooth objective-function landscape with a well-defined minimum, indicating that this regime supports stable and meaningful parameter optimization. In contrast, optimization for the High-Speed cluster did not converge, likely due to the limited data density in this extreme region of the parameter space (only 38 observations) or to strong nonlinearities in this regime, a behavior that is consistent with the difficulties of global and local optimization in multimodal and sparsely sampled spaces (Zhang; Glezakou, 2021).

The results reveal fundamental trade-offs among the clusters, summarized in Figure 6. The Conventional cluster offers the highest reliability (92.2% success rate) but moderate productivity, whereas the High-Feed cluster maximizes material removal rate at the expense of higher cutting force (352.2 N versus 147.8 N) and reduced success rate (62.2%). This quality–force trade-off is in agreement with previous multi-objective studies on Ti6Al4V turning, which also report that improvements in surface finish and productivity are commonly accompanied by increased mechanical loads on the tool (Nguyen et al., 2023; Gutema et al., 2022).

Figure 6. Radar chart comparing the three clusters in four critical dimensions: roughness (inverted), productivity, success rate, and force (inverted).

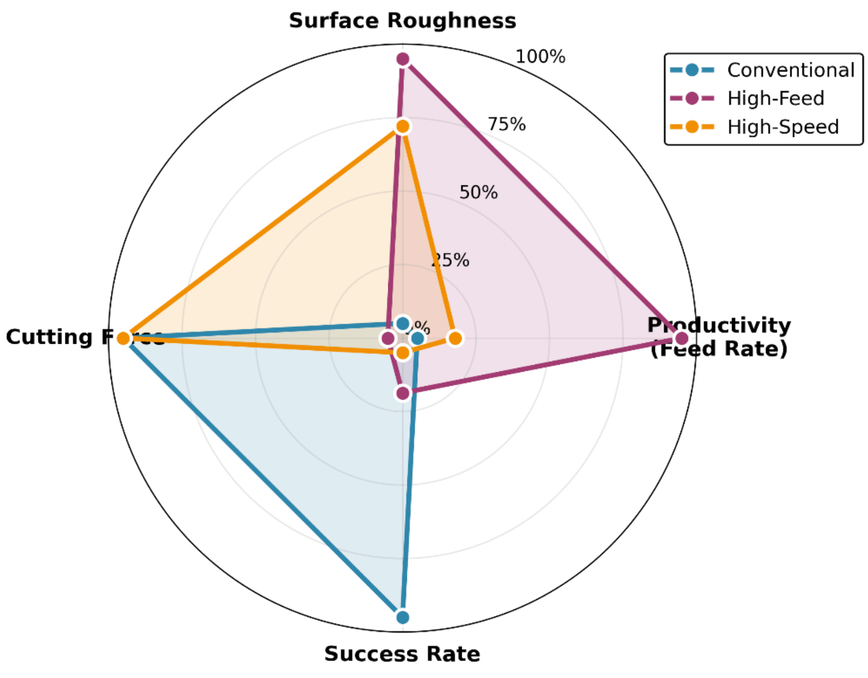

Source: Authors (2026).

Based on these findings, the following industrial recommendations are proposed:

- For critical operations where reliability and consistent quality are required: use parameters from the Conventional cluster (vc = 60–100 m/min, f = 0.08–0.12 mm/rev).
- For roughing or productivity-driven operations: adopt High-Feed strategies (vc = 80–120 m/min, f = 0.15–0.20 mm/rev) with strict tool-wear monitoring.
- High-Speed conditions should be applied cautiously and require additional experimental validation before industrial implementation.

The analysis also showed that feed force (Ff) had 2.3 times higher predictive importance than traditional cutting parameters, suggesting that real-time monitoring of this variable may provide better surface-quality indicators than conventional parameter control.

The cluster-based approach significantly outperformed global optimization methods, which produced suboptimal recommendations by ignoring data heterogeneity. However, the low R^2 value of the roughness model (0.0324) indicates that unmeasured factors—such as tool condition, machine vibrations, or material microstructure—have a strong influence on surface quality.

The qualitative classification of tool wear ("Low," "Medium," and "High") proved insufficient for quantitative modeling, suggesting that future studies should incorporate quantitative wear metrics (e.g., VB and KT) to improve model accuracy, in line with recent data-driven wear characterization approaches (Nguyen et al., 2023). In addition, the lack of direct temperature measurements (only Tchip available) limits a full thermo-mechanical interpretation of the process.

Cross-validation was performed by comparing model predictions with the three experimental trials closest to each optimal solution, showing acceptable agreement given the inherent variability of machining processes

5. Conclusion

This study developed and validated a cluster-based multi-objective optimization methodology for dry machining of Ti-6Al-4V, addressing the limitations of traditional optimization techniques when dealing with complex and heterogeneous experimental data.

Based on the analysis of 287 experimental trials, three distinct operational regimes were identified, representing different industrial machining strategies.

The main findings show that the Conventional cluster (vc = 70.0 m/min, f = 0.080 mm/rev) provides the highest reliability (92.2% success rate) with a mean surface roughness of 37.25 µm, making it suitable for critical operations where stability and consistent quality are required. The High-Feed cluster (vc = 80.0 m/min, f = 0.200 mm/rev) achieves higher productivity with slightly lower roughness (35.21 µm), but at the cost of significantly higher cutting forces (352.2 N) and a reduced success rate (62.2%), making it more appropriate for roughing operations.

The cluster-based approach proved superior to global optimization methods, which were inadequate due to nonlinear relationships and the coexistence of multiple machining regimes in Ti-6Al-4V cutting. Correlation analysis confirmed the complexity of the interactions, with feed force (Ff) exhibiting 2.3 times higher predictive importance than traditional cutting parameters, highlighting its potential as a real-time process monitoring variable.

REFERENCES

AMARAL, Bruno Vitiello do; SOUZA, Alex Fernandes de; PETRUCCI, Ellen Rodrigues de Oliveira; MELLO, Carlos Henrique Pereira; CAMPOS, Paulo Henrique da Silva. Análise de componentes principais para variáveis do processo de torneamento a seco. In: **ENCONTRO NACIONAL DE ENGENHARIA DE PRODUÇÃO (ENEGEP)**, 43., 2023, Fortaleza. *Anais*... Rio de Janeiro: ABEPRO, 2023. Disponível em: https://doi.org/10.14488/enegep2023_tn_wpg_399_1956_46257. Acesso em: 13 jan. 2026.

CHEN, Xuelin; TANG, Jinyuan; SHAO, Wen; HU, Bo; YE, Jinxiang. An analytical and experimental study on cutting characteristics and transient cutting force modeling in feed directional ultrasonic vibration-assisted cutting of high strength alloys. **Materials**, Basel, v. 15, n. 20, art. 7388, 2022. Disponível em: https://doi.org/10.3390/ma15207388. Acesso em: 13 jan. 2026.

GUTEMA, Endalkachew Mosisa; GOPAL, Mahesh; LEMU, Hirpa G. Minimization of surface roughness and temperature during turning of aluminum 6061 using response surface methodology and desirability function analysis. **Materials**, Basel, v. 15, n. 21, art. 7638, 2022. Disponível em: https://doi.org/10.3390/ma15217638. Acesso em: 13 jan. 2026

KLIPPEL, Hagen; SÜSSMAIER, Stefan; ZHANG, Nanyuan; KUFFA, Michal; WEGENER, Konrad. Large-scale investigation of dry orthogonal cutting experiments Ti6Al4V and Ck45. **The International Journal of Advanced Manufacturing Technology,** London, v. 135, p. 2871–2908, 2024. Disponível em: https://doi.org/10.1007/s00170-024-14597-2. Acesso em: 13 jan. 2026.

LIU, Dewei; LI, Changhe; DONG, Lan; QIN, Aiguo; ZHANG, Yanbin; YANG, Min; GAO, Teng; WANG, Xiaoming; LIU, Mingzheng; CUI, Xin; ALI, Hafiz Muhammad; SHARMA, Shubham. Kinematics and improved surface roughness model in milling. **The International Journal of Advanced Manufacturing Technology**, London, v. 131, p. 2087–2108, 2024. Disponível em: https://doi.org/10.1007/s00170-022-10729-8. Acesso em: 13 jan. 2026.

NGUYEN, Van-Hai; LE, Tien-Thinh; LE, Minh Vuong; MINH, Hoang Dao; NGUYEN, Anh-Tu. Multi-objective optimization based on machine learning and non-dominated sorting genetic algorithm for surface roughness and tool wear in Ti6Al4V turning. **Machining Science and Technology**, London, v. 27, n. 4, p. 380–421, 2023. Disponível em: https://doi.org/10.1080/10910344.2023.2235610. Acesso em: 13 jan. 2026.

SHARMA, Antriksh; CHEN, Jie; DIEWALD, Evan; IMANIAN, Anahita; BEUTH, Jack; LIU, Yongming. Data-driven sensitivity analysis for static mechanical properties of additively manufactured Ti–6Al–4V. **Journal of Risk and Uncertainty in Engineering Systems, Part B: Mechanical Engineering**, New York, v. 8, n. 1, art. 011108, 2022. Disponível em: https://doi.org/10.1115/1.4051799. Acesso em: 13 jan. 2026.

SOUZA, Alex Fernandes; SOUZA, Luiz Leonardo; GAUDÊNCIO, João Henrique D.; *et al.* Wear classification in Ti6Al4V machining using explainable machine learning: a decision support approach. **Journal of the Brazilian Society of Mechanical Sciences and Engineering**, Cham, v. 48, art. 103, 2026. Disponível em: https://doi.org/10.1007/s40430-025-06078-8.

ZHANG, Jun; GLEZAKOU, Vassiliki-Alexandra. Global optimization of chemical cluster structures: methods, applications, and challenges. **International Journal of Quantum Chemistry**, Hoboken, v. 121, n. 3, e26553, 2021. Disponível em: https://doi.org/10.1002/qua.26553.